Hyperfine Interact
DOI 10.1007/s10751-013-0860-3

Structural, calorimetric and magnetic properties study of the $Cu_{0,91}Fe_{0,09}O$ system

H. D. Colorado · J. S. Trujillo Hernandez · G. A. Pérez Alcázar · Alberto Bolaños

Abstract In this work the $Cu_{0.91}Fe_{0.09}O$ nanocrystalline system was prepared via the co-precipitation method. Using Mössbauer Spectrometry, X-Ray Diffraction, Vibrating Sample Magnetometry, Thermogravimetry and Differential Scanning Calorimetry, we study the magnetic behavior, and the structural and calorimetric properties of this system. X-ray diffraction shows only the presence of the CuO structural monoclinic phase, suggesting that Cu atoms are substituted by Fe ones. This hypothesis was confirmed by Mössbauer spectrometry at room temperature, because it shows that the spectrum is formed by two doublets, which correspond to Fe^{+2} and Fe^{+3} sites. Hysteresis cycles obtained by vibrating sample magnetometry detect a soft ferromagnetic behavior at room temperature with coercive fields between 8 and 20 Oe. At T = 20 K the sample shows a hard-magnetic behavior. The thermogravimetry results show a Néel temperature ($T_N > 440$ °C). The differential scanning calorimetry curve show two endothermic peaks in the 90–120 °C range.

Keywords Mössbauer spectrometry · X-ray diffraction · Vibrating sample magnetometry · CuO

1 Introduction

Magnetism in nanoparticles is currently the subject of interest because of its wide application in industrial as well as research areas [1]. CuO, as a narrow band gap p-type semiconductor, has been recognized as an industrially important material for

Proceedings of the Thirteenth Latin American Conference on the Applications of the Mössbauer Effect, (LACAME 2012), Medellín, Columbia, 11–16 November 2012.

H. D. Colorado (✉) · J. S. T. Hernandez · G. A. P. Alcázar
Departamento de Física, Universidad del Valle, Meléndez, A. A 25360 Cali, Colombia
e-mail: hernan.colorado@correounivalle.edu.co

A. Bolaños
Departamento de Química, Universidad del Valle, Meléndez, A. A 25360 Cali, Colombia

Published online: 24 April 2013

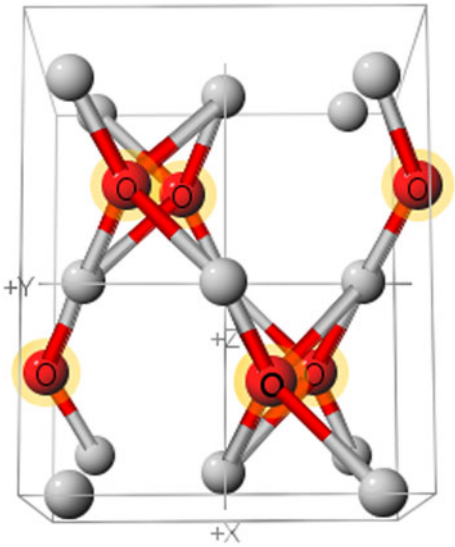

Fig. 1 Monoclinic structure of the CuO system. Image taked from the reference [13]

a variety of practical applications, such as gas sensors [2], catalysis [3], optics, solar energy conversion [4], and field emission [5]. CuO is antiferromagnetic bellow 230 K [6], but when it is doped at very low concentrations, it could exhibits anomalous magnetic properties [7, 8]. For this reason, it is interesting to know the response of this compound when it is doped with other materials, for example Fe. In recent years, ferromagnetism in semiconductors, including oxides, has received renewed attention, partly due to interest in spintronic device concepts, as spin valve for magnetic recording, sensor devices, spin transistors and nonvolatile storage devices, in which it can be controlled spin injection by weak magnetic field [9, 10]. CuO nanoparticles exhibit unique properties, such as ferromagnetic response due to the uncompensated surface spins, and an optical band gap (2.43 eV) which is larger than that of bulk CuO (1.85 eV). These surface spins are responsible for the observed anomalous magnetic properties of CuO nanoparticles [11]. For example, temperature dependent magnetic effects of the surface spin lead to several interesting phenomena such as enhanced magnetic moments, superparamagnetism, and magnetic hysteresis [12]. CuO presents a lattice with a monoclinic symmetry and a magnetic susceptibility temperature behavior that is unusual for 3d antiferromagnets. Each atom has four nearest neighbors of the other kind [13] (see Fig. 1). The bulk CuO is an antiferromagnetic material with Néel temperatures reported near 215 and 230 K. However, surface spins can dominate magnetization in nanostructures because of uncompensated exchange coupling. This may lead to ferromagnetic like behavior at low temperatures. In recent years, several studies on Fe-doped CuO nanomaterials have been reported [14–18].

In this work we study the structural, thermal, and magnetic behavior of Fe-doped CuO, taking into account its possible technological applications and the basic aspects of magnetism that are not understood in this system. In this work CuO samples doped with 9 % Fe are prepared using the co-precipitation method. This paper presents the magnetic behavior of the sample at 300 K and 20 K, studied by transmission Mössbauer spectrometry (MS) and hysteresis loops. The structural

properties were studied by X-ray diffraction (XRD). The thermal properties were studied by the thermogravimetry (TGA) and the differential scanning calorimetry (DSC) techniques.

2 Experimental method

The production process of copper monoxide doped with Fe was arisen by the co-precipitation method. We used stoichiometric amounts of Cupper Nitrate, $Cu(NO_3)3H_2O$ and Iron Nitrate, $Fe(NO_3)_39H_2O$. The starting salts were put in an aqueous solution under magnetic stirring at 600 rpm for 40 min at 40 °C. Then with the addition of Sodium Hydroxide (NaOH), co-precipitation occur releasing heat to stabilize and eventually kill a temperature of 40 °C. NaOH is used to control the PH which remained at 12.53 in the aqueous solution on magnetic stirring for 1 h. The resulting precipitate, from the chemical reaction, is slowly cooled to room temperature, and then transferred to a centrifuge at 2000 rpm for 10 min in order to decant the $Cu(FeOH)_2$ and remove the $NaNO_3$ formed. This process was repeated four times until the complete removal of $NaNO_3$. Then the precipitate was dried for 192 h at 50 °C and calcined for 5 h at 260 °C. A pure CuO sample was also produced by the same method. Mössbauer measurements were performed in a conventional spectrometer at room temperature with transmission geometry using a ^{57}Co source of 25 mCi in a Rh matrix. All spectra were fitted with the Mosfit program [19], and the isomer shift values are referred to that of α-Fe. The X-ray measurements were obtained using Cu-Kα radiation and the patterns were refined using the GSAS program [20], which is based in the Rietvelt method combined with Fourier analysis to describe the broadening of the lines. With this refinement the average values of the lattice parameter, crystallite size, and the structural phase were obtained. The behavior of the magnetization as a function of the field was studied by using the vibrating sample magnetometer (VSM) making use of a Physics Properties Measurement System (PPMS) equipment of the Excellence Center for New Materials (CENM). Surface morphology of the sample was observed using a scanning electron microscope (SEM) of the same center. The thermogravimetry (TGA) measurements were performed with a small applied field ($\approx$ 20 Oe) to determine the T_N as a function of temperature. The measurement was performed in N_2 atmosphere with a heating rate of 10 °C/min.

3 Results and discussion

Figure 2 shows the XRD patterns of the CuO and $Cu_{0.91}Fe_{0.09}O$ samples. It can be seen that both samples present a single monoclinic structural phase, and this confirms that all Fe atoms are substituting Cu atoms in the CuO lattice [18]. From the refinement of the diffractogram of CuO it was obtained that: the perpendicular and parallel crystallite sizes are equal to 51,4 $\pm$ 0,1 and 25,7 $\pm$ 1,3 nm, respectively, indicating that the crystallites have an elongated shape; and that the lattice parameters of this structure are a = 4,68 Å, b = 3,42 Å and c = 5,13 Å. From the diffractrogram of CuO doped with Fe it was found that: the perpendicular and parallel crystallite sizes are equal to 36,8 $\pm$ 0,2 nm and 40,4 $\pm$ 0,5 nm, respectively, showing that the

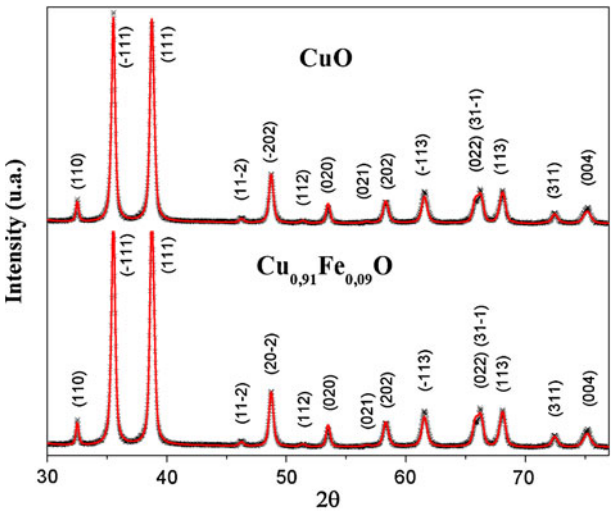

Fig. 2 XRD patterns of the $Cu_{0,91}Fe_{0,09}O$ system

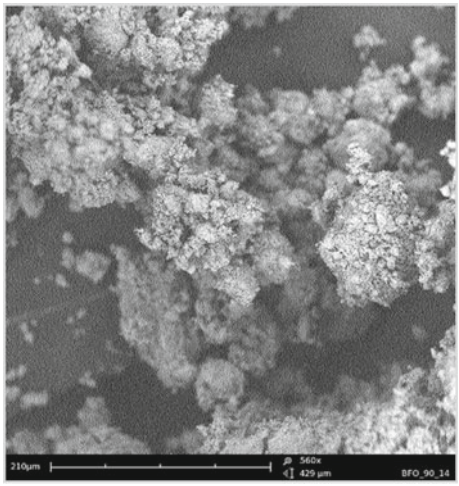

Fig. 3 SEM image (6100X) of the $Cu_{0,91}Fe_{0,09}O$ sample after calcination at 260 °C

crystallites have a nearly oblate shape; the lattice parameters of this structure are a = 4,69 Å, b = 3,41 Å and c = 5,13 Å. Comparing the lattice parameters of both samples it is observed that they do not vary significantly, indicating that there is no deformation of the lattice by the Fe doping. Additionally, it can be said that the reduction of crystallite size obtained due the replacement of Cu by Fe atoms produces a more fragile material.

According to the micrograph obtained by SEM, and shown in Fig. 3, it can be noted that the particles present an agglomeration tendency; this result is consistent with [11]. But the resolutions do not permit to obtain the mean particle size.

Figure 4 shows the Mössbauer transmission spectrum of the $Cu_{0,91}Fe_{0,09}O$ sample measured at room temperature. The Mössbauer spectrum was fitted with two doublets indicating the paramagnetic nature of the sample and the total dissolution of

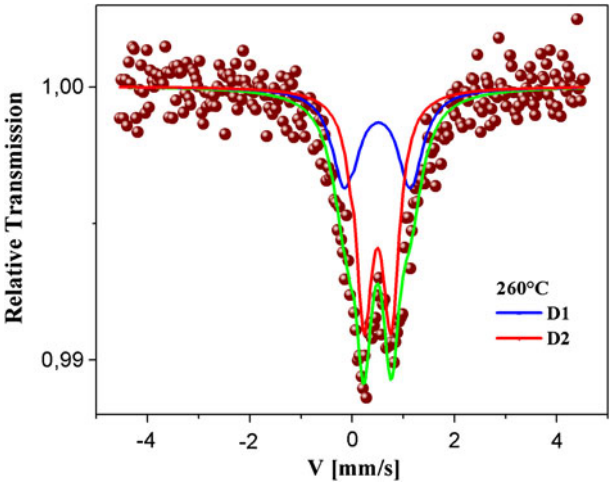

Fig. 4 Transmission Mössbauer spectrum of the $Cu_{0,91}Fe_{0,09}O$ system

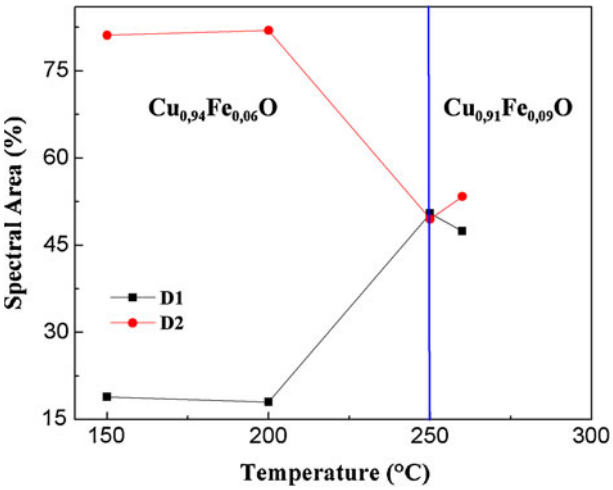

Fig. 5 Variation of the spectral area with the different calcinations temperatures of the $Cu_{0,94}Fe_{0,06}O$, results from reference [17] and compared with the current $Cu_{0,91}Fe_{0,09}O$ system

the Fe atoms, substituting Cu atoms. The doublets have a line half width of 0,50 mm/s showing a disordered paramagnetic behavior of the system. The two doublets present basically the isomer shift of the Fe^{+3} ($\delta = 0{,}35$ mm/s), but different quadrupole splitting ($\Delta Q_1 \cong 1{,}10$ mm/s and $\Delta Q_2 \cong 0{,}49$ mm/s, respectively). Then it is proposed that the second site (D_2) corresponds to a Fe^{+3} site and the first one (D_1) to the Fe^{+3} site but with a more asymmetric charge distribution around it.

Figure 5 presents the behavior of the spectral area of each doublet, with the calcination temperature; these data were compared with those of Ref. [17]. These authors reported the variation of the spectral area and of the quadrupole splitting with the different calcination temperatures of the $Cu_{0,94}Fe_{0,06}O$ system obtained at temperatures of 150, 200 and 250 °C. The fourth points plotted in Fig. 5 are the current data reported for the $Cu_{0,91}Fe_{0,09}O$ at a calcination temperature of 260 °C. It is observed that the D_2 area tends to increase with temperature while that of D1

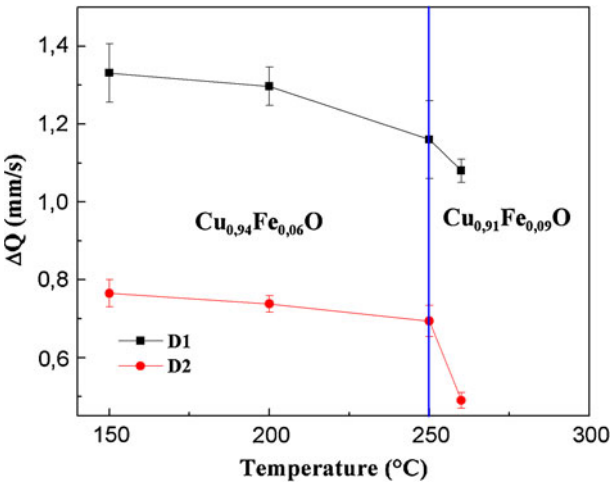

Fig. 6 Variation of the quadrupole splitting with the different calcinations temperatures of the $Cu_{0,94}Fe_{0,06}O$, results from reference [17] and for the present $Cu_{0,91}Fe_{0,09}O$ system are compared

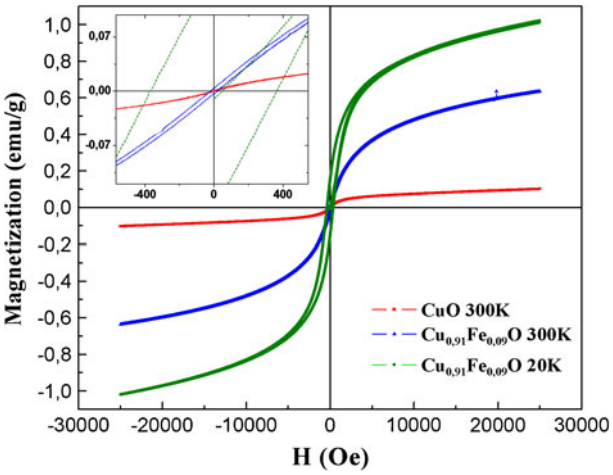

Fig. 7 Hysteresis loop of the $Cu_{0,91}Fe_{0,09}O$ system

decreases. Between 250 °C and 260 °C the diffusion of atoms due to the calcination temperature favors the Fe^{+3} site with the highest charge asymmetric than that of the other site.

In Fig. 6 the quadrupole splitting of both sites, obtained for different temperatures, are compared. It is observed that between 250 °C and 260 °C both values decrease, indicating that by increasing the calcination temperature and the Fe doping, a reduction of the asymmetry is obtained.

Magnetization measurements of both samples show a ferromagnetic behavior with coercive field of 8 ± 1 Oe for the CuO and 20 ± 1 Oe for the Fe-doped sample, as seen in Fig. 7. These magnetization curves were taken at $T = 300$ K and indicates a soft magnetic behavior of the material [21]. The Fe-doped sample measured at $T = 20$ K shows a coercive field of 372 ± 5 Oe indicating that there is a bigger ordering of magnetic moments due the temperature decrease. The increase in the field shows that the material behaves as magnetically hard at low temperatures.

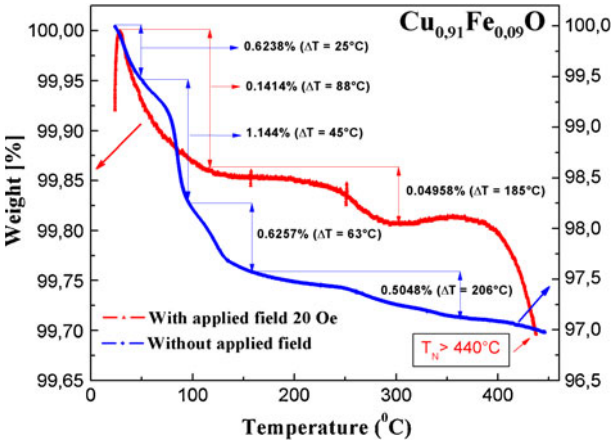

Fig. 8 Termogravimetry without applied field and with applied field of (≈ 20 Oe) of the $Cu_{0,91}Fe_{0,09}O$ system

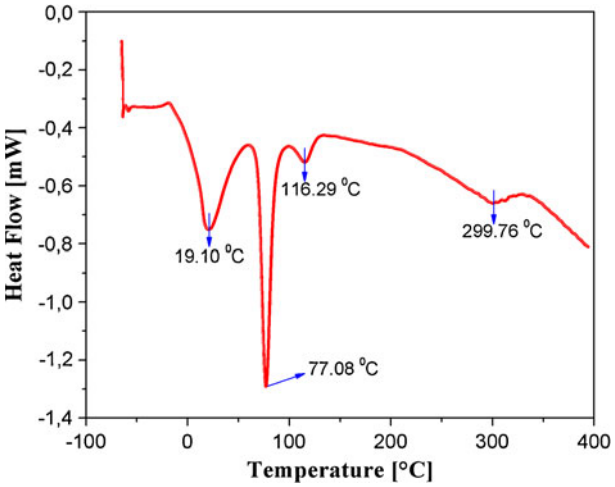

Fig. 9 Differential scanning calorimetry of the $Cu_{0,91}Fe_{0,09}O$ system

The different behavior shown by the Mossbauer (paramagnetic) and by hysteresis cycles (soft ferromagnetic) is a consequence of the different measurement times of both techniques. The hysteresis cycles in these samples are part of the anomalous behaviors which were also reported by other authors [12] and they attribute this behavior to the superficial spins.

In Fig. 8 the TGA measurement of the doped sample is shown. A weight loss of 3 % was obtained between room temperature and nearly 120 °C. Besides the maximum at 20 °C, small anomalies can be noted near 80 and 120 °C and these may be due to the evaporation of water and/or gases which are present at the surface of the sample. The water presence is a consequence of the hygroscopic character of the CuO. Two small anomalies can also be observed at around 250 and 400 °C.

Figure 8 also shows the effect of an applied field (≈ 20 Oe) on the thermogravimetric answer of the doped sample and it can be noted that the anomalies at 300 and 400 °C are enhanced, especially that at around 400 °C. We associated this anomaly

corresponds to a structural phase transition. This results show a Néel temperature ($T_N > 440$ °C), this result is consistent with [18].

In Fig. 9 the DSC measurement is shown and three endothermic peaks around 20, 80 and 120 °C are detected. They correspond to irreversible processes and agree with the anomalies detected for the loss of weight of Fig. 8 and correspond to the energy adsorbed by the sample to remove impurities, water or gas, on the sample surface. Additionally between 300 and 350 °C a change of curvature corresponding to a reversible processes can be attributed. However, this still needs to be checked with magnetic and XRD measurements at higher temperatures, in order to prove our proposal or to see if this anomaly corresponds to a structural phase transition.

4 Conclusions

XRD results indicate that the sample has a characteristic pattern of CuO, when Fe atoms replace Cu atoms. A decrease of the crystallite size is obtained with the addition of Fe. These DRX results indicate that the material is nanostructured and SEM micrograph proves that the particles are agglomerated. Transmission Mössbauer spectrometry results show that there is a disordered paramagnetic behavior due to the large value of the line half-width of the obtained doublets. The results obtained for the hysteresis loop indicate that the material at room temperature (300 K) shows a soft magnetic behavior, but by making measurements at 20 K this presents an ordering of magnetic moments which increases the coercive field indicating that the material has a hard magnetic behavior at this temperature.

References

1. Batlle, X., Labarta, A.: J. Phys. D **35**, R15 (2012)
2. Zhang, J., Liu, J., Peng, Q., Wang, X., Li, Y.: Chem. Mater. **18**(4), 867–871 (2006)
3. Teng, F., Yao, W., Zheng, Y., Ma, Y., Teng, Y., et al.: Sens. Actuators B, Chem. **134**, 761–768 (2008)
4. Anandan, S., Wen, X., Yang, S.: Mater. Chem. Phys. **93**, 35–40 (2005)
5. Hsieh, C.-T., Chen, J.-M., Lin, H.-H., Shih, H.-C.: Appl. Phys. Lett. **83**, 3383–3385 (2003)
6. Roden, B., Braun, E., Freimuth, A.: Solid State Commun. **64**, 1051–1052 (1987)
7. Borzi, R.A., Stewart, S.J., Punte, G., et al.: J. Appl. Phys. **87**, 4870–4872 (2000)
8. Bishta, V., Rajeeva, K.P., Banerjee, S.: arXiv:0911.1838v2 (2011)
9. Wolf, S.A., Awschalom, D.D., Buhrman, R.A., et al.: Sci., **294**, 1488–1495 (2001)
10. Fukimura, T., Yamada, Y., Toyosaki, H., et al.: Appl. Surf. Sci. **223**, 62–67 (2004)
11. Punnoose, A., Magnone, H., Seehra, M.S., Bonevich, J.: Phys. Rev. B. **64**, 174420 (2001)
12. Rao, G.N., Yao, Y.D., Chen, J.W.: IEEE Trans. Magn. **41**, 3409–3411 (2005)
13. Crystal lattice structures [On-Line]. http://cst-www.nrl.navy.mil/lattice/spcgrp/index.html. Accessed 5 Jan 2012
14. Li, Y., Xu, M., Pan, L., Zhang, Y., Guo, Z., Bi, C.: J. Appl. Phys. **107**, 113908 (2010)
15. Yin, S.Y., Yuan, S.L., Tian, Z.M., Liu, L., Wang, C.H., Zheng, X.F., Duan, H.N., Huo, S.X.: J. Appl. Phys. **107**, 043909 (2010)
16. Jing, Z., Qinglin, Z., Jinmin, L.: **33**(013001), 1–3 (2012)
17. Colorado, H.D., Pérez Alcázar, G.A.: Hyperfine Interact. **202**, 139–144 (2011)
18. Joseph, D.P., Venkateswaran, C., Vennila, R.S.: Adv. Mater. Sci. Eng. **2010**, 1–4 (2010)
19. Teillet, J., Varret, F.: MosfitProgramm, University du Maine, unpublished, (1976)
20. Larson, A.C., Von Dreele, R.B.: General Structure Analysis System (GSAS), Los Alamos National Laboratory Report LAUR, pp. 86–748 (1994)
21. O'Handley, R.C.: Modern Magnetic Materials. Wiley, New York (1999)